

Structural characterization of nanogranular BaTiO₃-NiFe₂O₄ thin films deposited by laser ablation on Si/Pt substrates

J.R. Gonçalves, J. Barbosa, P. Sá, J.A. Mendes, A.G. Rolo, B.G. Almeida
 Dep. Física, Universidade do Minho, Campus de Gualtar, 4710-057 Braga, Portugal
 bernardo@fisica.uminho.pt

Multiferroic thin films constructed by mixing magnetostrictive and piezoelectric materials have attracted recently much scientific and technological interest [1]. In addition to possessing ferroelectricity and magnetism in each individual phase, they are shown to exhibit a stress mediated coupling between their magnetic and electric properties, the so called magnetoelectric effect [1]. Thus, the properties and performance of these nanostructures depend critically on the phase morphology and internal stress distribution, which, in turn, are determined by the elastic phase/phase and phase/substrate interactions. Here, nanogranular thin films composed by BaTiO₃ (piezoelectric) and NiFe₂O₄ (magnetostrictive) have been prepared, and their structural properties were characterized. The BaTiO₃-NiFe₂O₄ thin films were deposited by laser ablation, on platinum covered Si(001) substrates. The depositions were done with a KrF excimer laser (wavelength $\lambda = 248$ nm), at a fluence of 2 mJ/cm². The oxygen pressure was 1 mbar and the substrate temperature was 650°C. The ablation targets were obtained by sintering NiFe₂O₄ and BaTiO₃ powders with different concentrations. Structural studies were performed by X-ray diffraction (XRD), using a Philips PW-1710 diffractometer with CuK α radiation. Raman studies were performed using a Jobin-Yvon T64000 spectrometer.

Figure 1 shows the X-ray diffraction spectra measured on the nanocomposites with cobalt ferrite concentrations in the range 30% - 50%. For comparison, the end members BaTiO₃ and NiFe₂O₄ are also shown. The films are polycrystalline and composed by a mixture of tetragonal-BaTiO₃ and NiFe₂O₄ with cubic inverse spinel structure. As the concentration of the nickel ferrite increases the relative intensity of the (311) NiFe₂O₄ peak increases, indicating the progressive more oriented growth of this phase. The grain sizes, obtained from the fitted X-ray diffraction peak widths for both phases, were determined by using the Scherrer equation. They are in the range 20 - 71 nm for the barium titanate phase and 15 - 22 nm for the NiFe₂O₄ one.

The lattice parameters a and c of the tetragonal BaTiO₃ phase were obtained from the (200) and (002) peak positions. For the pure barium titanate film, a is slightly expanded and c is slightly contracted relative to the bulk, giving a lower tetragonal distortion of the BaTiO₃ structure. However, on the nanocomposites studied, the a and c lattice parameters of the BaTiO₃ phase are always above the bulk ones (but with c/a near the bulk one), indicating an overall expansion of the unit cell due to the presence of NiFe₂O₄. On the other hand, the lattice parameter of the NiFe₂O₄ phase, obtained from the (311) peak position, is always above the bulk value ($a_{\text{bulk}} = 4.339\text{\AA}$) and varies from 8.606 Å on the sample with lower cobalt ferrite concentration ($x=30\%$), to 8.624 Å on the sample with higher NiFe₂O₄ content ($x=50\%$). Comparing with the bulk NiFe₂O₄, in the films the nickel ferrite unit cell has an expansion strain that increases as its concentration increases, up to $x=50\%$.

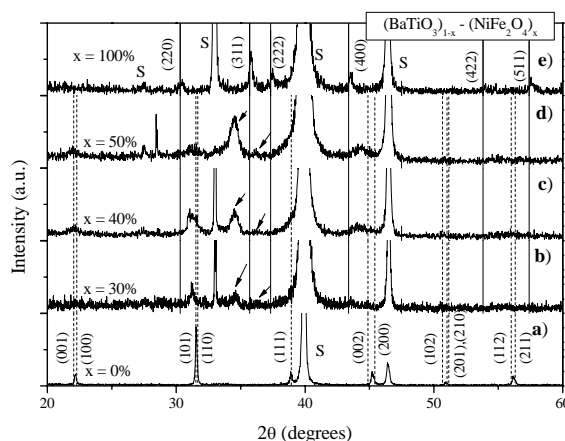


Figure 1: X-ray diffraction spectra of the samples deposited with nickel ferrite concentrations $x = 0\%$ - 50% and 100% . The peaks marked with an S are from the substrate.

Figure 2 shows the Raman spectra of the thin film samples deposited with cobalt ferrite concentrations in the range 30%-50%. Also shown are the individual BaTiO_3 and NiFe_2O_4 bulk reference powders, for comparison. In the BaTiO_3 case, the peak at 716 cm^{-1} , corresponds to the longitudinal optical (LO) vibration of the E phonon mode [2] and the decrease of its intensity with increasing nickel ferrite concentration reflects the corresponding decrease of the barium titanate content in the films.

The inverse spinel structure of AFe_2O_4 consists of AO_6 and FeO_4 octahedra and FeO_6 tetrahedra. The modes arising from the octahedra and tetrahedra can be easily distinguished in the Raman spectrum of ferrites. Raman peaks over the region $660\text{--}720\text{ cm}^{-1}$ represent the modes of tetrahedra and those in $460\text{--}660\text{ cm}^{-1}$ region correspond to modes of octahedra [3]. The nickel ferrite modes appearing at 570 cm^{-1} and 700 cm^{-1} can then be assigned to octahedral site (O-site) sublattice and tetrahedral site (T-site) sublattice vibration modes, respectively [3].

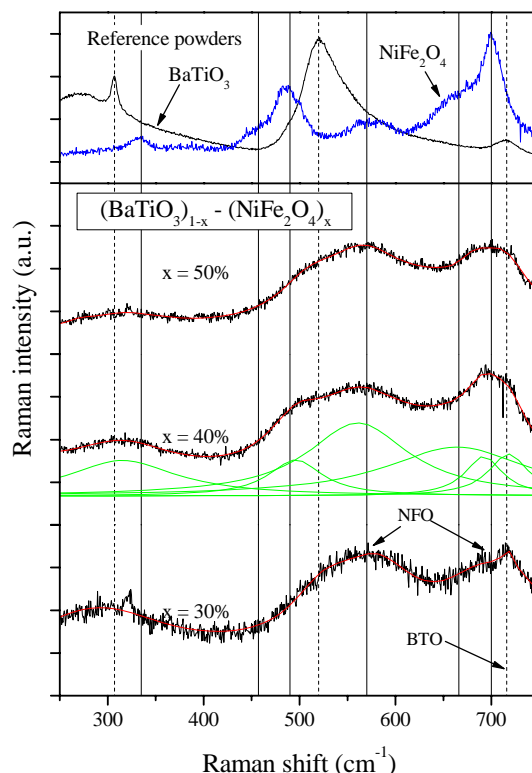


Figure 2: Raman spectra of the samples deposited with NiFe_2O_4 concentrations in the range 30%-50%, along with the corresponding fitting curves. Also shown are the BaTiO_3 and NiFe_2O_4 reference powders, and the Lorentzians obtained from the fit to the spectrum of the sample with $x = 40\%$.

Based on the peaks observed on the powders, the nanocomposite films spectra were

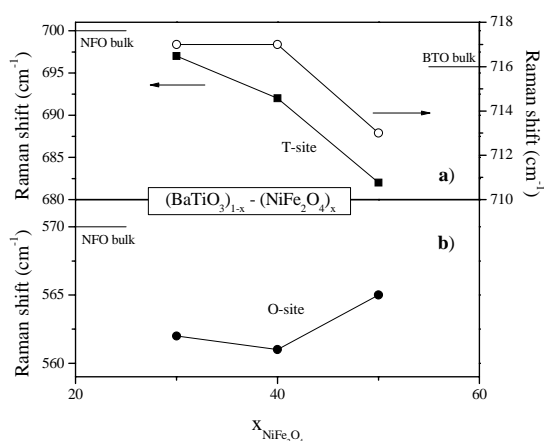


Figure 3: Raman shift as a function of the NiFe_2O_4 concentration, for the a) left: O-site and b) T-site modes. In the right axis of a) is the E mode of BaTiO_3 which appears at 716 cm^{-1} in the bulk.

deconvoluted by using Lorentzian line-shape functions to least-squares fit the Raman peaks (fig. 2). Figure 3 shows the vibrational modes wavenumbers for the O-site and T-site Raman peaks of the NiFe_2O_4 phase as well as of the BaTiO_3 phase E peak near 716 cm^{-1} . As the nickel ferrite concentration increases, the barium titanate E peak of figure 3 is near and somewhat oscillates around the bulk value. On the other hand, the NiFe_2O_4 T-site mode has a redshift on the nanocomposites, with its wavenumber being systematically below the bulk value. A similar trend is observed for the O-site mode, for the films with 40% and 50% NiFe_2O_4 concentration. This redshift of the NiFe_2O_4 modes results from the expansion of the lattice parameter of the nickel ferrite, as was similarly observed from the X-ray diffraction results (fig. 1).

References:

- [1] - W. Eerenstein, N. D. Mathur, J. F. Scott, *Nature*, **442** (2006) 759
- [2] - U.V. Venkateswaran, V.M. Naik and R. Naik, *Phys. Rev. B*, **58** (1999) 14256
- [3] - S.P. Sanyal, R.K. Singh, "Phonons in condensed materials", Allied Publishers, (2004)